Intra-Body Backscattering for Wearable Ring Sensor

Noor Mohammed*, Robert W. Jackson*, Sunghoon Ivan Lee†, Jeremy Gummeson*
*Electrical and Computer Engineering, University of Massachusetts Amherst, MA, USA
†College of Information & Computer Science, University of Massachusetts Amherst, MA, USA
Email: noormohammed@umass.edu, jackson@ecs.umass.edu, silee@cs.umass.edu, jgummeso@umass.edu

***Abstract*—This paper presents a novel human-body communication technology that enables capacitive intra-body backscatter (C-IBB) communication between a batteryless ring sensor and a wrist-worn transceiver. C-IBB leverages the finite conductivity of human skin and air coupling capacitance to facilitate near-field communication (NFC) between wearable devices. The C-IBB system features a radio frequency energy harvester connected to an impedance-matched wearable electrode, which charges a capacitor. This energy storage capacitor powers an ultra-low-power microcontroller, enabling backscatter communication by modulating the electrode's load impedance. In this work, we developed a modular heterodyne transceiver system and intra-body channel gain emulator. These tools optimize transceiver and tag systems for realistic channel gains tailored to specific electrode configurations. We validated the system's performance on the human body, optimizing it for sensing applications in a wearable ring format. Our preliminary study reveals that the system supports a bit rate of 20.83 kbps with a bit error rate of 10^{-3} to 10^{-2} and operates effectively within a range of 23 cm.**

***Index Terms*—Wireless power transfer, backscatter communication, human body communication (HBC), intra-body power transfer, intra-body communication.**

I. Introduction

Backscatter communication is an energy-efficient wireless communication method that operates on electromagnetic energy reflection due to load impedance modulation from the transponders [1]. This technique accommodates wide frequencies, making it applicable for both near-field and far-field sensing applications. It allows low-power sensing systems to communicate with remote transceivers without generating secondary carrier signals from the sensing node. Therefore, backscattering communication can facilitate sustainable communication within ultra-low-power sensor networks.

In this work, we implement and study backscatter communication in the human body using a capacitive link. Capacitive intra-body backscatter (C-IBB) communication is a technique that utilizes the unique properties of the human body, such as its conductivity and permittivity, along with its surrounding environment, to facilitate communication between a skin-coupled, batteryless sensor, and a transceiver. This technology promises to enable a new generation of batteryless, ultra-low-power wearable sensors, offering a significant advantage over traditional active radio technologies like bluetooth low-energy (BLE).

BLE has been widely adopted in wearable devices such as rings or ear sensors. However, it relies on active radio frequency (RF) transmission at 2.4 GHz for advertising, synchronization, and packet overhead, which consumes considerable energy and makes long-term batteryless operation infeasible [2]. Moreover, the high attenuation of 2.4 GHz signals through human tissue leads to unreliable performance in body-coupled scenarios, often requiring increased transmit powers in the range of 4 dBm to 10 dBm [3]. In addition, BLE performance is significantly degraded by co-channel interference from Wi-Fi traffic, since both share the crowded 2.4 GHz ISM band [4]. Finally, continuous exposure to 2.4 GHz radiation near the skin causes tissue heating in long-term use cases [5].

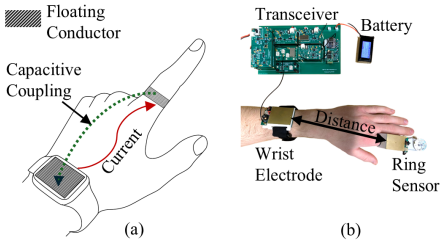

Fig. 1. Batteryless sensor operated through intra-body power transmission. (a) Illustrates the intra-body loop formed via the air and skin path, and (b) shows a prototype of an intra-body batteryless sensor system.

In contrast, our proposed C-IBB system avoids active microwave radiation, leverages direct electrode–skin coupling without requiring any complex antenna design, and making it inherently more energy-efficient, and safer by adopting operating frequency of 40 MHz.

Prior works on body coupled communication extensively looked at the human body as a power bus to enable energy exchange between devices placed at distant body locations [6]. In C-IBB applications, the primary goal is to maximize the coupling capacitance between the skin-coupled electrode system in the near field. This is achieved through the integration of a isolated balun transformer and resonant impedance matching with the electrodes [7].

Unlike conventional wireless communication systems, a C-IBB system requires careful consideration of the intra-body channel's loop gain, which encompasses both forward (S_{21}) and reverse (S_{12}) transmission gains since a C-IBB sensor tag rely on the carrier signal transmitted by the transceiver for both power and data transmission. Previous studies [7], [8] have highlighted that the intra-body path gain is highly sensitive to the air coupling capacitance between floating conductors in the electrode system, as shown in Fig. 1(a). This introduces several challenges in developing practical

This work is supported in part by the NSF under Grant No. 016419-00001 and NIH under Grant No. R01HD114147.

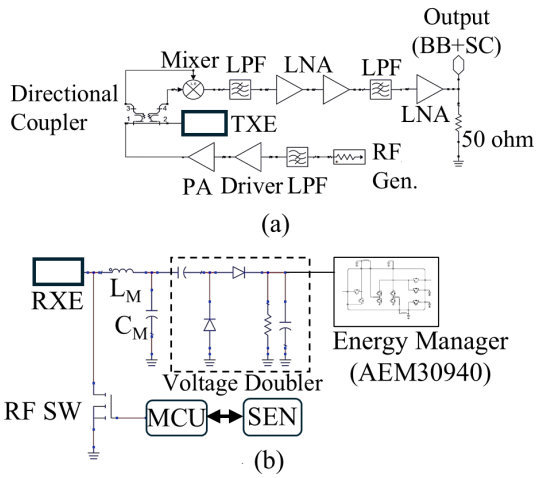

Fig. 2. Schematic diagram of the C-IBB (a) transceiver front-end, and (b) sensor tag.

intra-body backscatter communication applications since air coupling capacitance is in the femtofarad (fF) range [8], which can cause significant gain fluctuations in the near field.

A prior study on intra-body power transfer model [8] reveals that the path gain can be approximated as a fixed attenuation for a specific carrier frequency and range – i.e. the gain response for the impedance matched electrodes remains constant for a narrow frequency band. Similar approximations are also used in the gain estimation of aperture coupled microstrip patch antennas where authors modeled air path losses using a fixed attenuator [9]. Therefore, it is reasonable to model the intra-body channel gain using a discrete-valued RF attenuator — this simplifies hardware development while minimizing measurement errors induced by increased air coupling capacitance from the unintentional grounding effects of benchtop equipment. This hardware based gain simplification offers a low-cost tool that facilitates the development of body coupled transceivers.

In this work, we design a modular transceiver and a batteryless sensor that enables the development and implementation of intra-body backscatter communication systems. While similar systems have been used by industry for studying unidirectional gain, our design is the first to enable backscatter communication between a wearable transceiver and a batteryless ring sensor.

II. Hardware System

The proposed C-IBB hardware system consists of a transceiver, electrode system, and a batteryless ring sensor. The following section describes the the major hardware components.

A. Transceiver

Figure 2(a) shows the schematics of the transceiver front end. Here, the output port of the coupler is connected to the wrist electrode (TXE). Figure 3(a) shows the implemented transceiver hardware with gain emulator and batteryless sensor tag. The transceiver consists of an RF transmitter and a receiver. The transmitter module includes a microcontroller,

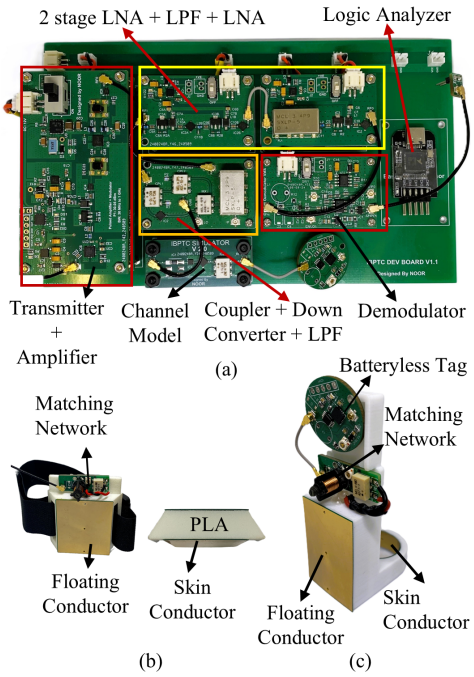

Fig. 3. (a)The C-IBB Transceiver Hardware System with gain emulator and batteryless ID tag, (b) wrist electrode, and (c) ring electrode with batteryless sensor tag.

frequency synthesizer (RF Gen.), low-pass filter (LPF), a driving amplifier (Driver), and a power amplifier (PA) delivering 28.5 dBm of peak RF power at 40 MHz. The transmitter operates with a 33 % duty cycle when interrogating the C-IBB batteryless sensor tag, which helps reduce average power consumption. During the interrogation cycle, the transmitter simultaneously powers the tag and listens for the backscattered signal. Depending on the available channel gain, the C-IBB transceiver employs multiple short carrier pulses to charge the storage capacitor before listening for a response from the tag. A higher channel gain requires fewer pulses to complete the backscatter cycle for a given storage capacitor.

The receiver includes a directional coupler, a frequency downconverter with a passive mixer, two stages of LPF to attenuate the 40 MHz carrier, and three stages of low noise amplification (LNA) for improving the signal-to-noise ratio (SNR) of the down converted signal.

The output port in the receiver chain in Fig. 2(a) is connected to the demodulator module as shown in Fig. 3(a). The demodulator processes the modulated 1 MHz subcarrier (SC) signal to recover the baseband (BB) signal. The BB signal processing chain consists of an envelope detector, non-inverting ac coupled amplifiers, and a pulse shaper circuit to convert the baseband signal to a digital bitstream. The bitstreams are recorded with a logic analyzer connected to a host computer.

In Fig. 3(a), the implemented channel gain model consists of a -36 dB RF attenuator and DC-DC isolating balun to isolate the tag ground from the transceiver ground. Through our experiments, we found that the average channel gain is approximately -36 dB for 10 cm body channel length (i.e.,

wrist-to-hand channel) where the channel length is defined as an edge-to-edge distance between the wrist and finger electrodes as shown in Fig. 1(b). We used this model to characterize the sensor tag's energy consumption. However, during physical layer evaluation of the intra-body channel, we replaced the channel gain emulator with electrodes (See Fig. 1(b)) placed on human participants.

B. Batteryless Sensor Tag

The C-IBB sensor tag in Fig. 3(c) comprises five sub-modules: the impedance matching circuit, a voltage doubler using SMS7630 schottkey diodes, a power management IC (AEM30940), an ultra-low power microcontroller (PIC16LF1823), and an RF switch (ADG902) as a carrier modulator. Figure 2(b) shows the schematics of the tag system. Here, RXE represents the skin coupled receiving electrode, RF SW is the CMOS switch, and SEN represents the sensor. An LC network is used to impedance match the charge pump and its load to 50 $ohms$ at -10 dBm, 40 MHz RF. The output of the charge pump is connected to the input of the power management IC (PMIC). The PMIC features a DC-DC boost-buck converter along with a low drop-out regulator (LDO) to supply a stable DC voltage to the microcontroller (MCU) and the modulator circuit. The PMIC charges a 94 μF storage capacitor to 4.12 V, while the LDO provides a stable 1.8 V. This setup enables the MCU to generate a baseband signal combined with a 1 MHz subcarrier, which acts as a switching signal for a high-speed CMOS switch within the modulator. The output of the modulator is connected to the impedance matching circuit, which modulates the incoming 40 MHz RF carrier signal. This results in the reflected or backscattered signal within the intra-body loop.

C. Electrode System

Figure 3(b) shows the wrist electrode and Fig. 3(c) shows the ring electrode system. Each electrode has a DC-DC isolation balun and 50 ohm impedance matching network optimized for dry-skin coupling. The wrist electrode's dimension is 30 $mm \times 40$ mm where the skin and floating conductors are separated by a 11 mm thick polylactic acid (PLA) substrate [8]. The finger electrode has a top conductor of 20 $mm \times 30$ mm, while the skin conductor is a strip of width 10 mm integrated inside a ring of 20.6 mm diameter.

III. Results

In this section, we evaluate the physical layer of the proposed C-IBB system through analyzing the relationship between SNR and electrode separation distance (See Fig. 1(b)) to determine its effective operating range. Here, range is defined as maximum electrode separation distance. Next, we analyze the Bit Error Rate (BER) relative to electrode separation distance to show communication accuracy. Finally, we measure the sensor tag's power consumption, affirming C-IBB's suitability for ultra-low-power wearable sensor application.

Five male participants, aged 23–46 years with body mass indices (BMI) ranging between 22 to 43, were recruited for the study. The study protocol was approved by the Institutional Review Board of the University of Massachusetts Amherst (IRB #2909), and all participants provided written informed consent. Experiments were conducted in a laboratory environment at 19–27 °C and 40–60% relative humidity. Subjects were seated on plastic chairs with forearms resting on a desk to ensure consistent electrode placement and to minimize motion artifacts. All jewelry and metallic accessories were removed prior to testing. Electrodes were placed on the left wrist and index finger (See Fig. 1).

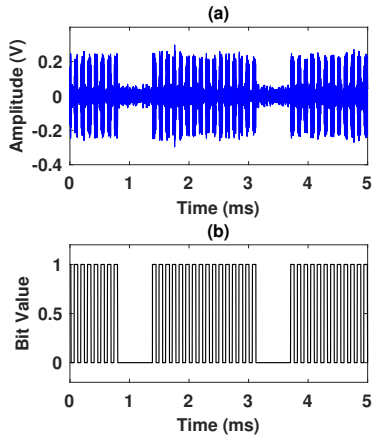

Fig. 4. Outputs observed from a human subject using ring configuration for a range of 23 cm where (a) shows received subcarrier and baseband signals, and (b) shows the recovered bit information.

In order to evaluate the physical layer, we programmed the sensor tag to generate a 1's and 0's (i.e. 1010...10) binary packet with 32-bit length, 48 μs bit duration, and 500 μs packet interval. To obtain the SNR of the transceiver, we recorded the raw baseband signal (as shown in Fig. 4(a)) using a battery operated digital storage oscilloscope (part: OWON VDS6102). The data from the oscilloscope was saved on a battery-operated laptop (part: Lenovo Chrome Book 11.6 inch) using a USB cable for offline processing.

The SNR was calculated from frequency-domain data obtained through a Fast Fourier Transform of the time-domain signal. The single-sided power spectrum was computed, and the signal bandwidth was identified using the 3 dB points around the spectral peak. Signal power was integrated within this bandwidth, while noise power was estimated from the mean power outside the signal bandwidth. The SNR was then calculated as the ratio of total signal power to average noise power.

To study the BER, a second-order Butterworth bandpass filter centered at 1 MHz (0.9–1.1 MHz passband) was applied on the raw baseband signal. A thresholding operation converted the filtered waveform into a sequence of 1's and 0's as shown in Fig. 4(b). Then, bit transitions were counted to evaluate the bit error rate.

A. SNR vs Range

Figure 5 shows the SNR study data obtained from five human (S-1 to S-5). Here, subject 1's (S-1) SNR drops from

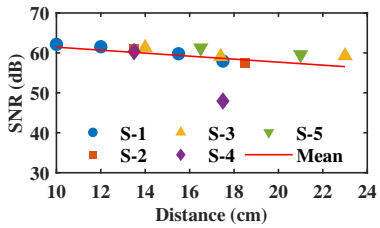

Fig. 5. SNR vs Distance data obtained from five human participants.

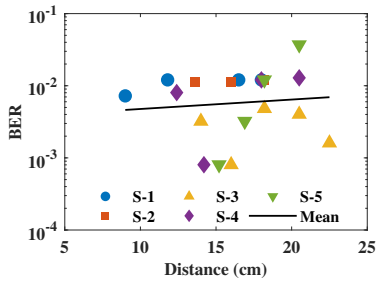

Fig. 6. BER vs Distance data obtained from five human participants.

62.15 dB at 10 cm to 57.96 dB at 17.5 cm. Subject 3 (S-3) maintains a SNR of 59.28 dB at highest range of 23 cm, while Subject 4 (S-4) experiences a significant drop.

The results confirm an inverse relationship between communication range and SNR while revealing substantial individual variability, likely due to anatomical differences, positioning, and surrounding complex dielectric environment during measurements.

B. *BER Study*

Figure 6 shows the BER results obtained from five human participants (S-1 to S-5). Subjects 1, 2, and 4 (S-1, S-2, S-4) showed a slight increase in BER of about $1.2\,\%$ at longer distances. Subject 3 (S-3), however, maintained a low BER of under $0.5\,\%$ even at extended distances, demonstrating excellent signal integrity. In contrast, Subject 5 (S-5) experienced a significant BER increase at 20.5 cm, indicating considerable signal attenuation. The transmitted bits are typically in the order of kilobits due to the limited energy available for passive backscattering. This resulted in bit error rate in the order of 10^{-3} to 10^{-2}.

The analysis clearly indicates robust intra-body backscatter communication, with low BER values (approximately $0.5\,\%$–$1.5\,\%$) across most subjects and ranges. These results indicate the individual variability in intra-body communication performance. While short-range intra-body backscatter can achieve highly reliable communication, longer ranges may require personalized system calibration.

C. *Energy Consumption*

The energy consumption of the tag was obtained using the storage capacitance, operational voltage window programmed by the power manager, and number of bits generated by the tag within a single packet burst. As the bit duration increased from 10 µs to 48 µs, the total number of transmitted bits decreased significantly, from 6,912 bits to 2,674 bits. Consequently, the energy consumption per bit rises, increasing from approximately 23.84 nJ/bit at the shortest duration to about 61.61 nJ/bit at the longest duration of 48 μs.

This highlights a direct trade-off between communication speed and energy efficiency. Shorter bit durations lead to better energy efficiency per bit, making them ideal for energy-constrained intra-body backscatter systems. On the other hand, longer bit durations may enhance robustness against channel impairments, but they do so at the expense of increased energy usage per transmitted bit.

IV. Discussion

This work presents a detailed physical-layer characterization of an intra-body backscatter communication system. Experimental results reveal an inverse relationship between communication range and signal strength, with the SNR range of 62 dB to 59 dB over short ranges of 10 cm to 23 cm and showing subject-dependent variability.

BER analysis indicates that participants generally performed well, with BER values as low as 0.5% in optimal cases. However, some subjects show elevated BERs at relatively longer ranges, indicating adaptive calibration needs.

Future work will concentrate on developing full-stack communication protocols to implement capacitive intra-body backscatter system in low powered wearable devices. We propose developing a custom Medium Access Control and application-layer protocol, inspired by EPC Gen2 but tailored for capacitive body channels. This protocol will include reader-driven queries, dynamic power management, self-clocked encoding (e.g., FM0), and lightweight error correction. These improvements will ensure efficient, reliable, and low-latency operation in energy-constrained body sensor network.

References

[1] A. P. Sample, D. J. Yeager, P. S. Powledge, A. V. Mamishev, and J. R. Smith, "Design of an RFID-based battery-free programmable sensing platform," *IEEE transactions on instrumentation and measurement*, vol. 57, no. 11, pp. 2608–2615, 2008.

[2] B. Martinez, M. Monton, I. Vilajosana, and J. D. Prades, "The power of models: Modeling power consumption for iot devices," *IEEE Sensors Journal*, vol. 15, no. 10, pp. 5777–5789, 2015.

[3] E. Wen, D. F. Sievenpiper, and P. P. Mercier, "Channel characterization of magnetic human body communication," *IEEE Transactions on Biomedical Engineering*, vol. 69, no. 2, pp. 569–579, 2021.

[4] H. Pirayesh, P. K. Sangdeh, and H. Zeng, "Coexistence of wi-fi and iot communications in wlans," *IEEE Internet of Things Journal*, vol. 7, no. 8, pp. 7495–7505, 2020.

[5] I. C. on Non-Ionizing Radiation Protection *et al.*, "Guidelines for limiting exposure to electromagnetic fields (100 khz to 300 ghz)," *Health physics*, vol. 118, no. 5, pp. 483–524, 2020.

[6] E. R. Post, M. Reynolds, M. Gray, J. Paradiso, and N. Gershenfeld, "Intrabody buses for data and power," in *Digest of Papers. First International Symposium on Wearable Computers*. IEEE, 1997, pp. 52–55.

[7] N. Mohammed, R. W. Jackson, S. I. Lee, and J. Gummeson, "A capacitive backscatter system for intra-body identification," *IEEE Journal of Radio Frequency Identification*, 2025.

[8] N. Mohammed, R. W. Jackson, J. Gummeson, and S. I. Lee, "Wireless intra-body power transfer via capacitively coupled link," in *2022 IEEE-EMBS International Conference on Wearable and Implantable Body Sensor Networks (BSN)*. IEEE, 2022, pp. 1–4.

[9] A. E. Lamminen, J. Saily, and A. R. Vimpari, "60-GHz patch antennas and arrays on LTCC with embedded-cavity substrates," *IEEE Transactions on Antennas and Propagation*, vol. 56, no. 9, pp. 2865–2874, 2008.